Journal of Colloid and Interface Science 643 (2023) 305–317

Contents lists available at ScienceDirect

Journal of Colloid And Interface Science

journal homepage: www.elsevier.com/locate/jcis

Specific ion effects on the aggregation of polysaccharide-based polyelectrolyte complex particles induced by monovalent ions within Hofmeister series

Makoto Yamazaki [a], Makoto Yabe [b], Kazutoshi Iijima [c,*]

[a] Graduate School of Engineering Science, Yokohama National University, Tokiwadai 79-5, Hodogaya-ku, Yokohama 240-8501, Japan
[b] Mol Processing, 1015 1-9-7 Kitashinagawa, Shinagawa-ku, Tokyo 140-0001, Japan
[c] Faculty of Engineering, Yokohama National University, Tokiwadai 79-5, Hodogaya-ku, Yokohama 240-8501, Japan

GRAPHICAL ABSTRACT

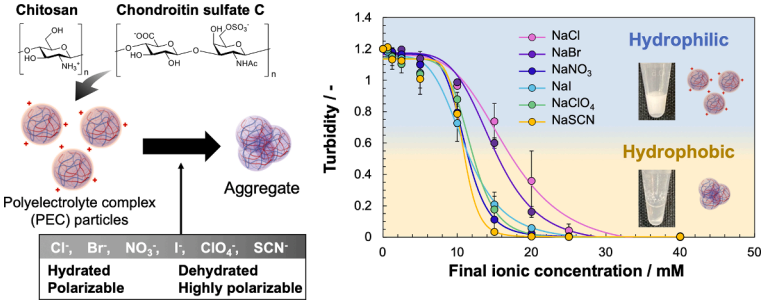

ARTICLE INFO

Keywords:
Polyelectrolyte complex
Chitosan
Chondroitin sulfate
Aggregation
Hofmeister series
Molecular dynamics simulation

ABSTRACT

Polysaccharide-based polyelectrolyte complex (PEC) particles have been utilized as carriers for drug delivery systems (DDS) and as building components for material development. Despite their versatility, the aggregation mechanism of PEC particles in the presence of salts remains unclear. To clarify the aggregation mechanism, the specific ion effects of monovalent salts within the Hofmeister series on the aggregation behavior of PEC particles composed of chitosan and chondroitin sulfate C, which are often used as DDS carriers and materials, were studied. Here, we found that weakly hydrated chaotropic anions promoted the aggregation of positively charged PEC particles. The hydrophobicity of the PEC particles was increased by these ions. Strongly hydrated ions such as Cl^- are less likely to accumulate in these particles, whereas weakly hydrated chaotropic ions such as SCN^- are more likely to accumulate. Molecular dynamics simulations suggested that the hydrophobicity of PECs might be strengthened by ions due to changes in intrinsic and extrinsic ion pairs and hydrophobic interactions. Based on our results, it is expected that the control of surface hydrophilicity or hydrophobicity is an effective approach for controlling the stability of PEC particles in the presence of ions.

* Corresponding author.
E-mail address: iijima-kazutoshi-mh@ynu.ac.jp (K. Iijima).

https://doi.org/10.1016/j.jcis.2023.04.030
Received 30 December 2022; Received in revised form 14 March 2023; Accepted 8 April 2023
Available online 13 April 2023

1. Introduction

Polyelectrolyte complexes (PECs), which are sometimes referred to as polyion complexes, can be formed between oppositely charged polyelectrolytes (PEs) via electrostatic interactions by mixing the component solutions [1–3]. PECs can adopt a variety of morphologies, such as films [2,4], hydrogels [5], and coacervates [6], and have a wide range of applications in various scientific fields, including tissue engineering [7] and nanomedicine [8]. In particular, submicron-sized colloidal PEC particles obtained by mixing with extremely dilute solutions exhibit a neutralized core, and the outer shell mainly consists of excess PEs, which stabilize the colloids against aggregation [9–11]. Since the 1970s, PEC particles have fascinated scientists as a bridge between polymer science and colloidal science because they possess the properties of both macromolecular and colloidal particles [12]. In recent years, PEC particles have been applied in nanomedicine, such as in drug delivery systems (DDS), by utilizing their three-dimensional network structure [8]. PECs composed of biomaterials, especially naturally occurring polysaccharides, are expected to exhibit high biocompatibility and biodegradability [11]. Furthermore, specific cell targeting can be achieved by utilizing the physiological activities of polysaccharides [8]. For example, PEC particles constructed from chitosan (CHI) as a cationic polysaccharide and chondroitin sulfate as an anionic polysaccharide exhibit high biodegradability, low toxicity, and cell-targeting functionality [13] and are useful for drug and gene delivery [14,15]. In addition, the absence of chemical cross-linking agents reduces the toxicity and other undesirable effects of the reagents and preserves the native properties of the polysaccharides [8]. PEC particles can also be used as building components for the development of films and hydrogels [16,17].

However, it is difficult to functionalize materials in which polysaccharide PEC particles are prone to aggregation in salt solutions, such as phosphate-buffered saline (PBS) [17]. Although it is necessary to understand the aggregation mechanism to control the stability of polysaccharide PEC particles, this has not been completely elucidated. So far, the aggregation of PEC particles by ions has been attributed mainly to the decrease in electrostatic repulsion between particles owing to charge screening [18]. Recent studies have shown that the charge screening of colloidal particles by ions is affected by the hydrophilicity or hydrophobicity of particles [19]. In general, there are many hydrated ions, namely kosmotropic ions, in the intracellular environment [20], and they accumulate on the hydrophilic surface of particles and exclude them from the hydrophobic surface [19]. Kosmotropic ions are likely to adsorb onto hydrophilic colloidal particles and promote their aggregation [19]. Hence, whether colloidal particles are hydrophilic or hydrophobic has a significant effect on aggregation.

It is well known that the hydrophobicity of PEs increases in the presence of ions because PEs adopt more loopy and dense structures through the formation of extrinsic ion pairs [21,22]. Thus, it can be assumed that the hydrophilic domains in the PEC particles are reduced through the neutralization of excess charged functional groups by ions, and the hydrophobicity of the PEC particles is increased. Interestingly, the formation of PE counterion pairs is known to be specific to ionic species [22]. The specific interaction between counterions and macromolecules was observed over 100 years ago, and this phenomenon was named the Hofmeister effect [23]. The Hofmeister effect is the subset of specific ion effects that follows the Hofmeister series. For instance, the order of the Hofmeister series for anions is $Cl^- > Br^- > NO_3^- > I^- > ClO_4^- > SCN^-$, consistent with their hydration strength [24,25]. The Hofmeister effects, more concisely “specific ion effects”, have been observed in broader systems such as biological [26,27], polymer [28–30], colloidal [19,31], and non-aqueous systems [24,31]. Hofmeister-related phenomena have been attributed to the specific interactions between the ions and water molecules and their subsequent effects on the hydrogen bonding network of water. The ionic specific hydration was addressed by grouping ions into kosmotropic ions with strongly hydrated properties and chaotropic ions with weakly hydrated properties [32–34]. Several studies revealed that the hydration amounts of ions manifest the thickness and the amount of water of PE multilayer [35,36]. According to recent literatures, however, specific ion effects are also governed by the shape, size and the polarizability of ions [22], hydrophilicity/hydrophobicity of the solute–solvent interface [37], and the Lewis strength [38]. Moreover, these effects can be seen even in the absence of solvent [38]. Thus, a fundamental understanding of complicated specific ion effects including the Hofmeister effects has been rapidly developed in recent years. Nevertheless, there are only a few examples of the analysis of the specific ion effects on the aggregation of PEC particles. Recently, it has been found that the stability of synthetic polymer PEC coacervates is affected by specific ion effects because these ions alter the hydrophobic interactions within the PEC [35,39,40]. In addition, some groups have succeeded in elucidating the ion effects on the coacervation behavior of PEC using molecular dynamics (MD) simulations [41,42].

In this study, diverse monovalent anions; Cl^-, Br^-, NO_3^-, I^-, ClO_4^-, and SCN^-, and Na^+ as the constant counterion, were added to the positively charged CS/CHI particle dispersion, and the ion effects on the aggregation were systematically analyzed by combining experimental and simulation approaches. Anions were chosen as the ionic species because they exhibit stronger ion-specific effects than cations because of their greater polarizability range [24,25]. In most classifications of the Hofmeister series ions, Cl^- is characterized as hydrated and polarizable (kosmotropic) anions, and SCN^- as dehydrated and highly polarizable (chaotropic) anions [43]. Turbidity, dynamic light scattering, ζ-potential measurements, and hydrophobic domain detection were conducted to study the aggregation behavior of CS/CHI particles in response to variations derived from the unique properties and concentration of ions. As such, the major aim of this work is to elucidate the roles of the specific ion effects on the PEC particles and the aggregation behavior associated with changes in their hydrophobicity. In addition, the ion effects on the interaction between CHI and CS at the atomic level were analyzed using all-atom MD simulations to explain the microscopic experimental results.

2. Materials and methods

2.1. Reagents

CHI (molecular weight (M_W) 100 kDa, >80% deacetylation) from crab shells, chondroitin sulfate C (CS) sodium salt (M_W *ca.* 20 kDa) from shark cartilage, NaCl and NaBr were purchased from Nacalai Tesque Inc. (Kyoto, Japan). $NaNO_3$, NaI, $NaClO_4$, NaSCN, and Coomassie Brilliant Blue (CBB) G-250 dye were purchased from FUJIFILM Wako Pure Chemical Corp. (Tokyo, Japan). All the reagents and chemicals were used as received. Ultrapure water (18.2 MΩcm) was prepared using Direct-Q UV5 (Merck Millipore) and used in all experiments.

2.2. Preparation of CS/CHI particle dispersion

CS/CHI particle dispersions were prepared according to our previous reports [16,17]. CHI was dissolved in a 1.0 mg/mL acetic acid aqueous solution with ultrapure water at a concentration of 1.0 mg/mL. CS was dissolved in ultrapure water to a concentration of 1.0 mg/mL. The CS solution was added dropwise to the CHI solution, and CS/CHI particles were formed by magnetic stirring at 700 rpm for 15 min at room temperature. After stirring, the mixture was centrifuged at 4640*g* (Model 5200; KUBOTA Corp., Tokyo, Japan) for 10 min at room temperature to remove large gels. The supernatants were re-centrifuged at 21,130*g* for 30 min (Model 3700; KUBOTA Corp.) at room temperature and the supernatants were removed. Then, the precipitates were sonicated and redispersed in ultrapure water using a probe sonicator (VP-050 N, Taitec Corp., Saitama, Japan) at 80% power for 15 s. The kosmotorpic anion, acetate, existed in these systems, however, their effects are negligible

because its concentration is extremely low (refer the supplementary material).

2.3. Turbidity measurement of CS/CHI particle dispersion in the presence of ions

Salt solutions (50 μL) of varying concentrations were added to 50 μL of 46 or 23 mg/mL CS/CHI particle dispersion in a 1.5 mL microtube. The mixture was vortexed using a vortex mixer (HI-Tech Inc., Tokyo, Japan) for 10 s and then centrifuged using a microcentrifuge (PC-100, SPD Scientific Pte Ltd, Singapore) at 2000*g* for 10 s. The turbidity of the supernatant was measured at 500 nm using a UV–visible spectrophotometer (NanoDrop One, Thermo Fisher Scientific, Waltham, MA, USA) [44,45]. All measurements were performed three times, and the results are presented as the mean ± standard deviation. Plots of turbidity as a function of ionic concentration were fitted using a 4-parameter logistic function in Eq. (1).

$$f(x) = \frac{A_1 - A_2}{1 + (x/x_0)^p} + A_2 \quad (1)$$

The analysis was conducted using Origin (Pro), 2021 [46]. Each fit parameter in all systems is described in Tables S1 and S2. The critical coagulation concentration (CCC) was defined as the concentration at which the initial turbidity was halved and was calculated using Eq. (1).

2.4. Measurement of diameter and ζ-potential of CS/CHI particles

The diameter and ζ-potential of the CS/CHI particles were measured three times using a ζ-potential and particle size analyzer (ELSZ-2; Otsuka Electronics Co., Ltd., Osaka, Japan). The results are described as mean ± standard deviation. The diameter and ζ-potential of CS/CHI particles in the presence of ions were measured using the following procedure. Ultrapure water (600 μL), NaCl, or NaSCN solutions at a given concentration were added to 600 μL of 46 or 23 mg/mL CS/CHI particle dispersion. Then, the mixture was vortexed with a vortex mixer (Hitec Mixer) for 10 s and centrifuged for 10 s using a microcentrifuge (PC-100) at 2000*g* for 10 s. 1 mL of the supernatant was collected and re-dispersed using a probe sonicator (VP-050N, Taitec Corp.) at 30% output for 5 s. The diameter and ζ-potential of CS/CHI particles in the supernatant were measured. When the particles aggregated, no measurements could be performed.

2.5. Detection of the hydrophobic domain in CS/CHI particles.

The hydrophobic domains present in the CS/CHI particles were detected using the CBB G-250 dye. 650 μL of NaCl or NaSCN solution was added to 650 μL of a 2.5 mg/mL CS/CHI particle dispersion. After vortexing for 10 s with a mixer (Hitec Mixer), the mixture was centrifuged with a microcentrifuge (PC-100) for 10 s. 1.2 mL of supernatant was collected in a 5 mL microtube and 1.2 mL of 5 μg/mL CBB solution was added. The mixture was incubated for 10 min at room temperature. The absorption of CBB was monitored between 450 nm and 750 nm using a UV/vis spectrophotometer (V-560, JASCO Corp., Tokyo, Japan). The CS/CHI particles exhibited absorption at wavelengths between 450 and 750 nm. The absorption spectrum of CBB was evaluated by subtracting the absorption of the CS/CHI particles from the absorption of the CS/CHI particles mixed with CBB. The mixture was centrifuged at 20,630*g* for 30 min (Model 3700) at room temperature and the supernatants were collected. The absorption of supernatants was monitored at 600 nm using a UV/vis spectrophotometer (V-560). The loading efficiency of CBB was determined by using Eq. (2) where C is the dye concentration in the supernatants and C_0 means the initial dye concentration (2.5 μM).

$$\text{Loading efficiency}(\%) = 100 - \frac{C}{C_0} \times 100 \quad (2)$$

2.6. All-atom MD simulation

All-atom MD simulations of protonated CHI (CHI-NH_3^+) and CS in an aqueous solution with ions were performed using GROMACS 2021.3 [47]. CHI chains with 12 monosaccharide units were constructed by generating 12 units of glucose linked by β-1,4 glycosidic acid bonds using GLYCAM06 software [48] and replacing the–OH groups bonded to C-2 with ammonium groups (–NH_3^+) with the Avogadro package [49]. CS chains with 12 monosaccharide units were prepared as six units of *N*-acetyl-galactosamine-6-sulphate (GalNAc(6S)) linked β-1,3 to GlcA. All carboxyl groups in GalNAc(6S), GlcA, and sulfate groups in GalNAc were deprotonated using the Avogadro package. The initial structures of NO_3^-, ClO_4^-, and SCN^- were prepared using the Avogadro package. Topology files in the GROMACS format for CHI-NH_3^+ and CS were then generated using ACPYPE [50]. The topology files of NO_3^-, ClO_4^- and SCN^- were set to the same values as those in Refs. [51,52,53], respectively. The force field parameters of Na^+, Cl^-, Br^-, and I^- were obtained from the AMBER99SB [54] force field. TIP3P water molecules have been introduced for water [55].

In each system, five molecules of CHI-NH_3^+ and CS were placed in a box with a size of 15 nm × 15 nm × 15 nm. To investigate the effect of ions on the complexation of polysaccharides, CHI-NH_3 and CS were dissolved in water with 1, 10, 100, or 1000 mM NaX (X = Cl, Br, NO_3, I, ClO_4, and SCN).

Periodic boundary conditions were adopted, with a time step of 2 fs. The electrostatic interaction was calculated using the particle mesh Ewald (PME) method [56] with a cut-off of 12 Å, and the van der Waals (vdW) interaction was cut off at 12 Å. All bond lengths are constrained using the LINCS algorithm [57]. To maintain the temperature at 298 K, temperature coupling using velocity rescaling [58] with a stochastic term is employed. The pressure at 1 bar was controlled using the Parrinello-Rahman method with a coupling constant of 2.0 ps [59].

After equilibration by energy minimization using the steepest descent method [60] with 50,000 steps, each system was pre-equilibrated with a constant number of particles, volume, and temperature (*NVT*), and a constant number of particles, pressure, and temperature (*NPT*) ensembles for 100 ps. The MD simulation was performed for 100 ns. The vdW interaction energy was described using a standard 12–6 Lennard-Jones short-range potential, while the electrostatic interaction energy was calculated using a Coulombic short-range potential. For visualization and analysis, PyMOL26 (The PyMOL Molecular Graphics System; http://www.pymol.Org) [61] was used. The number of water molecules and ions, and the density of the simulation box in each system were shown in Tables S3-5.

3. Results

3.1. Characterization of CS/CHI particle dispersions

The diameters and polydispersity indexes of CS/CHI particles in dispersion at concentrations of 46 and 23 mg/mL were 829.1 ± 20.1 nm and 0.258 ± 0.011, and 689.5 ± 6.0 nm and 0.221 ± 0.019, respectively. The ζ-potentials of CS/CHI particles in dispersions at concentrations of 46 and 23 mg/mL were 31.3 ± 5.3 and 47.7 ± 0.3 mV, respectively.

3.2. Aggregation behavior of CS/CHI particle dispersion in the presence of ions

Fig. 1 shows the turbidity of the supernatant of the concentrated (46 mg/mL) and diluted (23 mg/mL) CS/CHI particle dispersions in the absence and presence of various ions. As the ionic concentration increased, the turbidity decreased in both the concentrated and diluted dispersions, indicating that the CS/CHI particles aggregated in the presence of ions (Figs. 1, S1 and S2). The CCC values of the concentrated

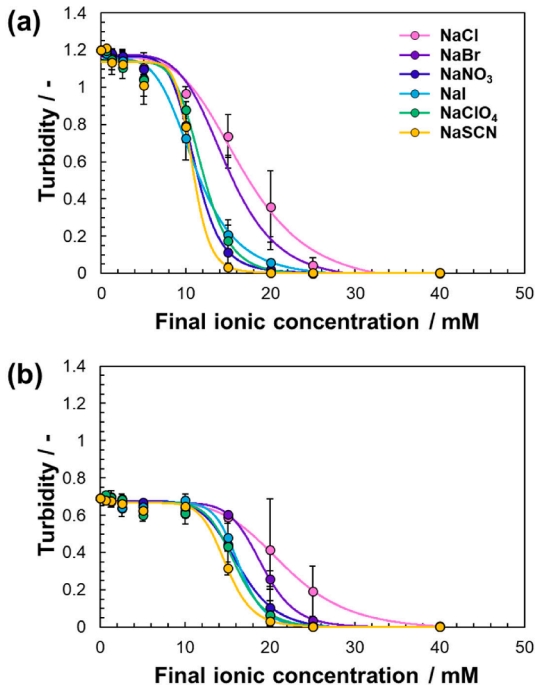

Fig. 1. Turbidity (absorbance at 500 nm) of 46 mg/mL (a) and 23 mg/mL (b) CS/CHI particle dispersion in the absence and presence of ions at different concentrations.

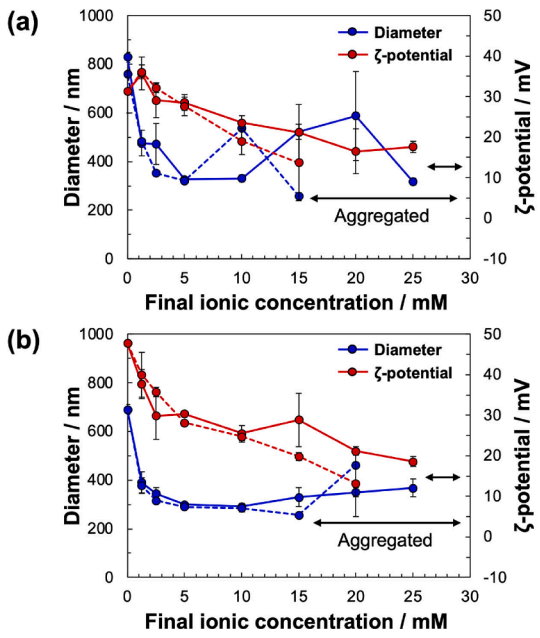

Fig. 2. Diameter and ζ-potential of CS/CHI particles at the concentration of 46 mg/mL (a) and 23 mg/mL (b) in the absence and presence of NaCl (solid line) or NaSCN (dotted line) at different concentrations.

and diluted CS/CHI particle dispersions, determined from the turbidity curve, are listed in Table 1. In concentrated CS/CHI particle dispersions, CCC follows the order $Cl^- > Br^- > NO_3^- = I^- = ClO_4^- = SCN^-$. In the diluted CS/CHI particle dispersion, CCC followed the order $Cl^- > Br^- > I^- = NO_3^- = ClO_4^- > SCN^-$. When comparing the same ionic species, the CCC in the concentrated dispersion was smaller than that in the diluted dispersion.

3.3. Diameter and ζ-potential of CS/CHI particles in the presence of ions

The specific ion effects on the diameter and ζ-potential of the CS/CHI particles in the supernatants were investigated in the presence of Cl^- as a kosmotropic anion and SCN^- as a chaotropic anion. For both concentrated and diluted dispersions, the diameter of the CS/CHI particles changed in the presence of ions (Fig. 2). For the CS/CHI particles in the concentrated dispersion containing NaCl, the diameter of the CS/CHI particles decreased at low concentrations (0–10 mM), increased at medium concentrations (10–20 mM), and decreased at high concentrations (20–25 mM). For CS/CHI particles in the concentrated dispersion containing NaSCN, the diameter decreased at low concentrations (0–5 mM), increased at medium concentrations (5–10 mM), and decreased at high concentrations (10–15 mM). For CS/CHI particles in the diluted dispersion containing NaCl, the diameter of the CS/CHI particles decreased at low concentrations (0–10 mM) and increased at high concentrations (10–25 mM). For CS/CHI particles in the diluted dispersion containing NaSCN, the diameter decreased at low concentrations (0–5 mM) and increased at high concentrations (15–20 mM).

For CS/CHI particles in the concentrated dispersion, the ζ-potential decreased in the presence of NaCl and NaSCN at concentrations above 2.5 mM. At concentrations of 10 and 15 mM, CS/CHI particles showed lower ζ-potential in the presence of NaSCN than in the presence of NaCl. For CS/CHI particles in the diluted dispersion, ζ-potential decreased in the presence of NaCl and NaSCN at concentrations above 1.25 mM. At concentrations of 15 and 20 mM, CS/CHI particles showed lower ζ-potential in the presence of NaSCN than in the presence of NaCl.

Table 1
Critical coagulation concentration (CCC) of various kinds of ions for the concentrated and diluted CS/CHI particle dispersion.

Ion	CCC/mM	
	46 mg/mL CS/CHI	23 mg/mL CS/CHI
Cl^-	16.4	21.6
Br^-	14.7	19.1
NO_3^-	11.1	16.2
I^-	11.0	16.3
ClO_4^-	11.8	15.9
SCN^-	10.8	14.8

3.4. Detection of the hydrophobic domain in CS/CHI particles

The loading efficiency of CBB dye as an indicator of the adsorbed amount in CS/CHI particles was analyzed. As shown in Fig. 3a, at low ionic concentrations, the loading efficiency of the CBB dye in CS/CHI particles with NaCl was higher than that with NaSCN. Meanwhile, at high ionic concentrations, the loading efficiency of dyes in CS/CHI particles with NaSCN was higher than that with NaCl. To detect the hydrophobic domain in CS/CHI particles in the supernatants, the maximum absorption wavelength (λ_{max}) of the CBB was determined from the absorption spectra of the mixture of CBB, CS/CHI particles, and NaCl or NaSCN (Fig. S3). As shown in Fig. 3b, λ_{max} of CBB in the presence of NaCl and NaSCN above a concentration of 1.25 mM was longer than that in the absence of ions. λ_{max} in 2.5 mM NaSCN solution was significantly higher than that in the presence of 2.5 mM NaCl. No significant change in the absorption spectra of CBB was observed depending on the ionic concentration of the system containing only CBB, NaCl, or NaSCN (Fig. S4).

3.5. All-atom MD simulation

Snapshots of CHI-NH_3^+ and CS at the end of the 100 ns MD simulation are shown in Figs. 4 and S5. The association between CHI-NH_3^+ and CS was observed in all systems after 100 ns of simulation within the adopted ionic species and ionic concentration. The polysaccharides constituting the complexes seem to become more loosely entangled as the ion concentration increases. The functions of ionic species and vdW

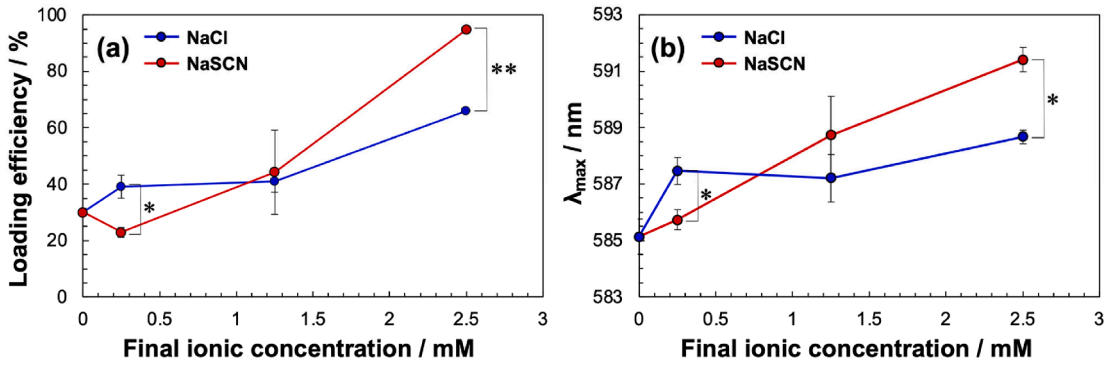

Fig. 3. (a) Loading efficiency of CBB in water upon adding CS/CHI particles. The CS/CHI particle dispersion (2.5 mg/mL) was mixed with NaCl or NaSCN solution, and the CBB solution was then added to the mixed solution to a final concentration of 2.5 μM. The mixture was centrifugated at 20,630 × g for 30 min at room temperature and the supernatants were collected. The absorption of supernatant was monitored at 600 nm with a UV/vis spectrophotometer. (b) Changes in the maximum absorption wavelength (λ_{max}) of CBB in the mixture of CBB, the CS/CHI particle dispersion, and the salt solution. The absorption of CBB was monitored between 450 and 750 nm with a UV/vis spectrophotometer. * indicates a significant difference (*p < 0.05, **p < 0.01, Student's *t*-test).

interaction energy calculated as the Lennard-Jones potential, electrostatic interaction energy, or the number of hydrogen bonds (H-bonds) between chains of CHI-NH_3^+ and CS were calculated (Figs. S6 and S8). The vdW interaction energy, electrostatic interaction energy, and H-bond number were generated over time, independent of the ionic concentrations and species. The mean values and standard deviations of each parameter plotted at 100 ns are shown in Fig. 5. The vdW interaction energy, electrostatic interaction energy, and H-bond number decreased in an ion-concentration-dependent manner. The order of the vdW interaction energy number and electrostatic interaction energy at 100 ns of the simulation was $Cl^- > NO_3^- > Br^- = I^- > ClO_4^- = SCN^-$ and $Cl^- > NO_3^- > Br^- = I^- = ClO_4^- > SCN^-$, respectively. The order of the H-bond number at 100 ns of the simulation follows $Cl^- > NO_3^- > Br^- = I^- = ClO_4^- > SCN^-$. To characterize the interactions between the extrinsic ion pair, intrinsic ion pair, and hydrophobic groups of the side chains, radial distribution functions (RDFs, *g* (r)) were calculated. Fig. 6 shows the RDFs of the anions surrounding $–NH_3^+$ of CHI-NH_3^+. The peak value decreased in a concentration-dependent manner regardless of the ionic species. Comparing the same ionic concentration, the peak values were larger in the system containing highly chaotropic ions, such as ClO_4^- and SCN^- than in systems containing kosmotropic ions, such as Cl^- and Br^-. Fig. 7 shows the RDFs of $–NH_3^+$ of CHI-NH_3^+ surrounding the $–OSO_3^-$ of CS in the presence of various ions at a given concentration. The peak value decreased in a concentration-dependent manner regardless of the ionic species. Comparing the same ionic concentration, the peak values were larger in the system containing highly kosmotropic ions, such as Cl^- and Br^- than in systems containing chaotropic ions, such as ClO_4^- and SCN^-. Fig. 8 shows the RDFs of C atoms at the 6-position of CS surrounding the C atoms at the 6-position of CHI-NH_3^+. Regardless of the ionic species, the peaks of the RDFs remarkably decreased in the presence of highly concentrated ions.

4. Discussion

The colloid aggregation has usually been examined based on turbidity changes [19]. Herein, the ion effects on the aggregation of CS/CHI particles were investigated by measuring the turbidity changes of the supernatants. Six different anions, Cl^-, Br^-, NO_3^-, I^-, ClO_4^-, and SCN^- were chosen to cover the gamut from kosmotropic to chaotropic [62]. The turbidity of the CS/CHI particle dispersion decreased in an ion concentration-dependent manner, suggesting the formation of aggregates of CS/CHI particles (Fig. 1). As shown in Fig. 2, the ζ-potential decreased as the ionic concentration increased, implying a decrease in electrostatic repulsion between the CS/CHI particles. This can be explained by the well-known Derjaguin-Landau-Verwey-Overbeek (DLVO) theory that the aggregation of colloids occurs by a reduction in electrostatic repulsion [63]. CCC of the anions varied depending on the ionic species (Table 1). In general, to analyze the specific ion effects, the ions are divided and contrasted among halide anions and polyatomic anions to avoid possible consequences arising from the specific geometries of the polyatomic ions [22,64]. Among the halide anions and polyatomic anions, the order of CCC of anions in both diluted dispersions was almost consistent with that of chaotropicity (Table 1), indicating that more highly chaotropic anions tend to cause the aggregation of CS/CHI particles. There is a large body of literature concerning Hofmeister effects on the soft matter such as polymers [30], micelles [43,65], and proteins [66,67]. For instance, the Hofmeister effects on the sol–gel transition temperature of thermosensitive polymers can be seen due to the ionic properties to stabilize or destabilize the hydrogen bonding between inter/intra molecular interaction within polymers [29,68]. In addition, Hofmeister effects on the critical micelle concentration (CMC) has been reported [43,65]. In the cationic surfactant, dodecyltrimethyl ammonium bromide (DTAB) system, the micelle formation is promoted by the chaotropic ions through the effective charge screening between head groups of surfactants and the release of the water around hydrophobic moieties [69]. Therefore, in simple terms, the order of CCC of our systems seems to be reasonable because the charge screening of particles would be promoted by chaotropic anions with high polarizability. However, the Hoffmeister effect on colloidal systems are extremely complicated, not so simple as mentioned above. In fact, Hofmeister effects in colloidal systems are strongly governed by the microscopic water structure around both the particle surface and the solvated ions. When the surface turns from hydrophobic to hydrophilic, an inversion of the Hofmeister series occurs [19,70,71]. For example, the CCC of positively charged hydrophobic colloids (latex) follows the Hofmeister series ($Cl^- > Br^- > NO_3^- > SCN^-$). In contrast, the CCC of positively charged hydrophilic colloids (triphosphate (TPP)/CHI) follows $SCN^- > NO_3^- > Cl^-$, which is reverse to that of the positively charged hydrophobic colloids. Considering that PEC particles generally exhibit a hydrophilic shell [8,72], chaotropic ions are expected to be excluded from the particles and kosmotropic ions promote aggregation. However, the actual results contradicted this expectation. The reason for this will be discussed later. In contrast, there was no difference in CCC among the polyatomic anions in the concentrated dispersions (Table 1). This may be due to the instability of the CS/CHI particles in the concentrated suspension. Colloidal particles are known to aggregate more easily at higher concentrations than at lower concentrations owing to the increase in the probability of particle–particle interactions, including hydrodynamic interactions and surface forces [73,74]. Therefore, the interaction between CS/CHI particles was enhanced in the concentrated dispersion and more easily aggregated in the presence of ions. The CCC in the concentrated dispersion was lower than that in the diluted

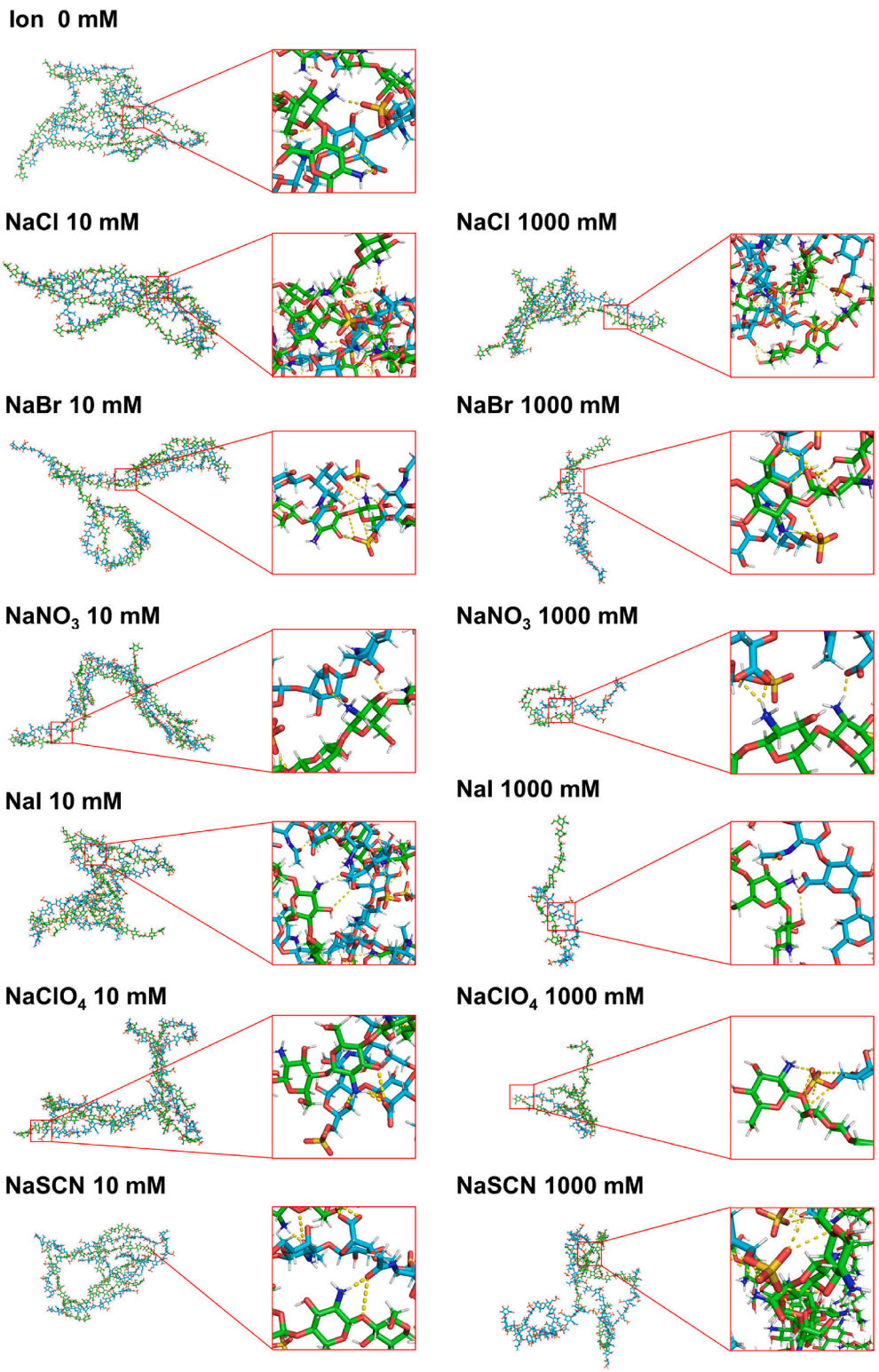

Fig. 4. Snapshots of CHI-NH_3^+ and CS in the absence and presence of various kinds of ions at the concentration of 10 mM and 1000 mM after 100 ns MD simulation (green stick chain: CHI-NH_3^+, blue stick chain: CS, blue: nitrogen, white: hydrogen, red: oxygen and orange: sulfur). Water and ion molecules were omitted for clarity. Enlarged atomic pictures of the interaction between CHI-NH_3^+ and CS were displayed in red solid line boxes. The H-bonds formed between CHI-NH_3^+ and CS are marked by red solid line boxes. (For interpretation of the references to colour in this figure legend, the reader is referred to the web version of this article.)

dispersion.

To examine the physicochemical changes during the aggregation of CS/CHI particles, DLS and ζ-potential measurements were performed. The diameter of the CS/CHI particles in the supernatants changed in an ion-concentration-dependent manner (Fig. 2). In both the concentrated and diluted dispersions, the diameter decreased under diluted salt conditions. This behavior can also be observed in water-soluble PECs [75]. This can be attributed to the shrinkage of polysaccharides from a stiff structure to a coiled structure because of the screening of electrostatic repulsion along the charged chains [75,76]. At medium and high ionic concentrations, the diameter of the CS/CHI particles increased in both the concentrated and diluted dispersions. This might be due to secondary aggregation between the primary particles caused by screening effects [77], as seen in the decrease in ζ-potential. Especially in concentrated dispersions, CS/CHI particles decreased in diameter in a highly concentrated salt solution. This could be explained by the

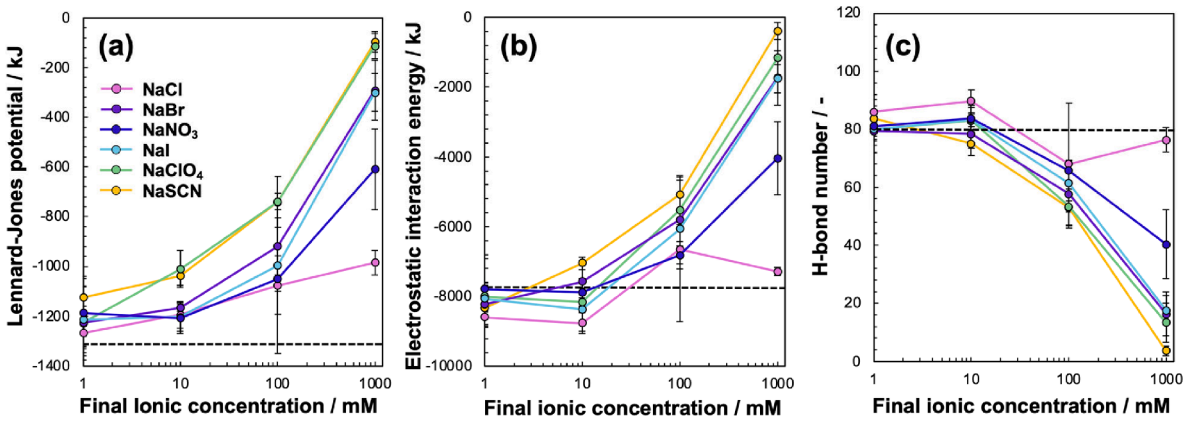

Fig. 5. Effects of the ionic strength on Lennard-Jones potential (a), electrostatic interaction energy (b), and H-bond number (c) between CHI-NH_3^+ and CS. The dotted line denotes the system values without ions.

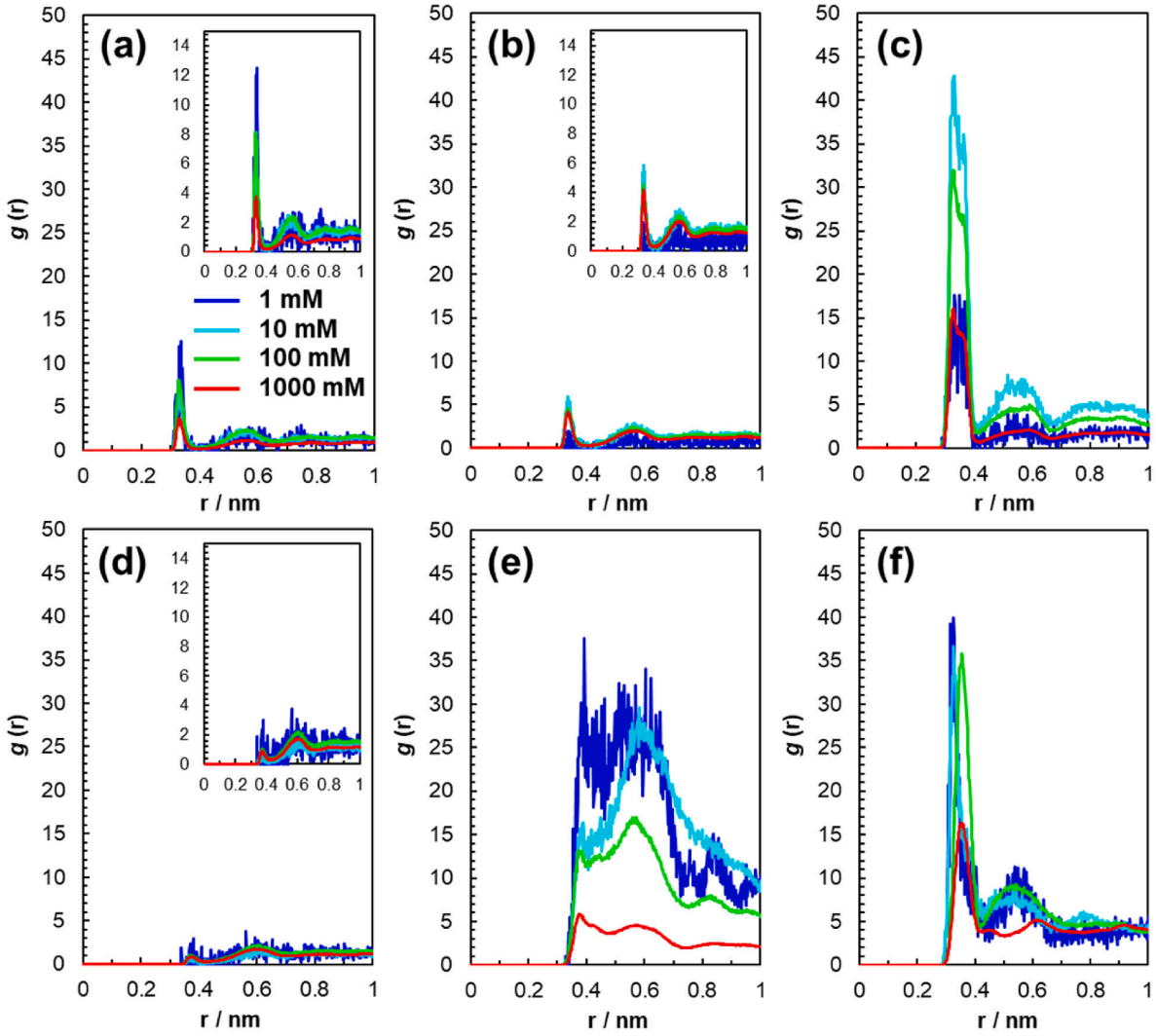

Fig. 6. RDFs of anions surrounding –NH_3^+ of CHI-NH_3^+ in the systems of CHI-NH_3^+ and CS with NaCl (a), NaBr (b), $NaNO_3$ (c), NaI (d), $NaClO_4$ (e), and NaSCN (f).

dissolution of PEC aggregates into small soluble complexes or partly by the PEC components [78,79]. This result is supported by the MD simulation results that the energy of the electrostatic interaction, which holds the PE chains together, decreased as the ionic concentration increased (Fig. 5b), implying that the electrostatic interaction was strongly screened by counterions [18]. In addition, the vdW interaction energy and number of H-bonds, which are also involved in the formation of PECs [80], decreased in a concentration-dependent manner (Fig. 5a, c).

The diameter of the ionic species increased at a lower ionic concentration in the NaSCN solution than in the NaCl solution (Fig. 2). This

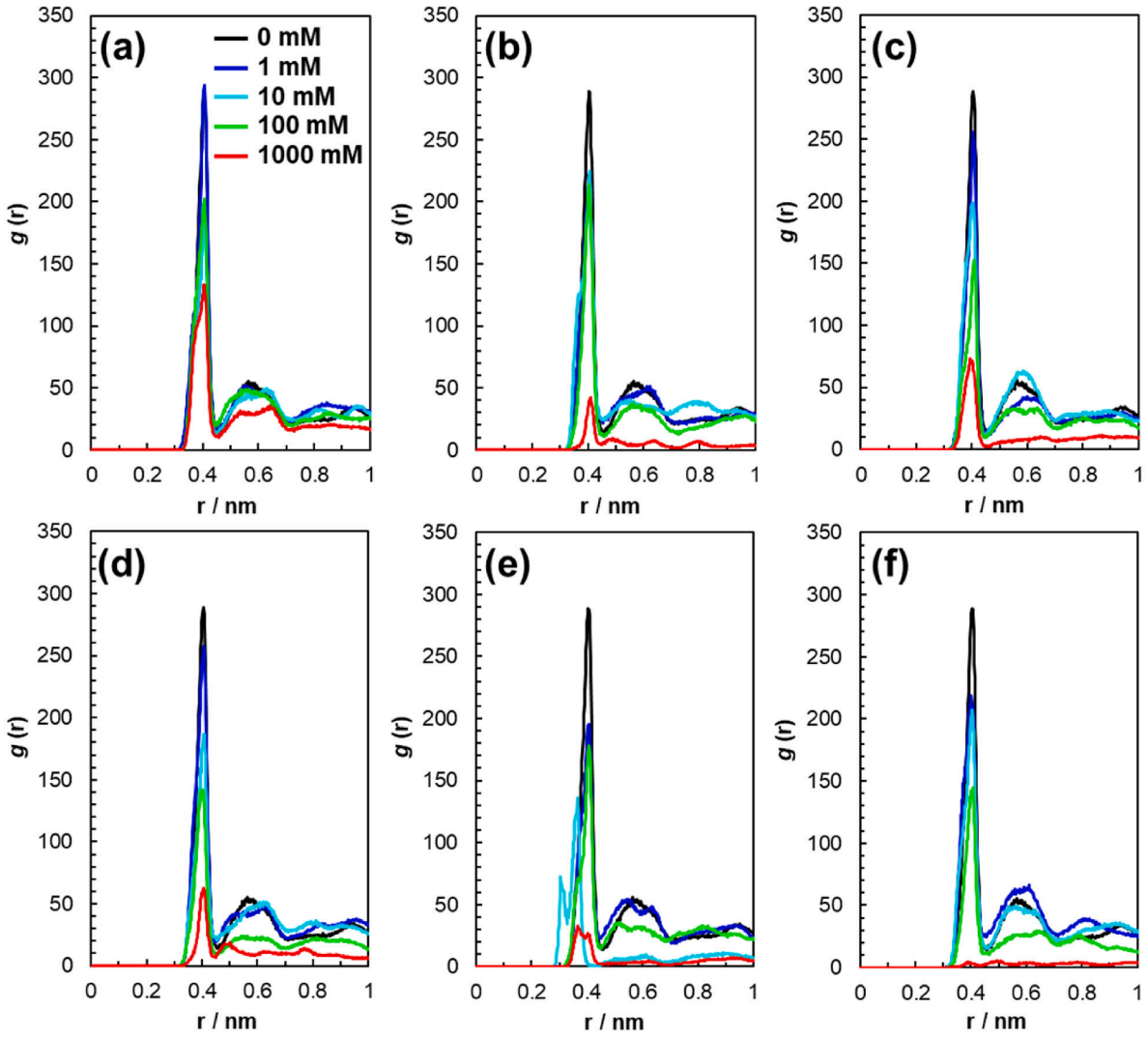

Fig. 7. RDFs of $-NH_3^+$ of CHI-NH_3^+ surrounding $-OSO_3^-$ of CS in the systems of CHI-NH_3^+ and CS with NaCl (a), NaBr (b), $NaNO_3$ (c), NaI (d), $NaClO_4$ (e), and NaSCN (f).

might be because the highly chaotropic anions, SCN^-, enhance the decrease in ζ-potential. As described below, CS/CHI particles become more hydrophobic in the presence of ions. Therefore, SCN^-, a weakly hydrated and highly chaotropic anion, is more likely to adsorb to the particles, neutralize the surface charge, and cause secondary aggregation. Considering that positively charged PEC particles composed of poly (sodium styrene sulfonate) (PSS) and polyallylamine (PAH) also tend to increase their particle size with highly chaotropic ions [81], it could be suggested that the specific ion effects on the diameter changes are commonly observed in both synthetic and biopolymer-based PECs. The decrease in the diameter of the CS/CHI particles in the concentrated dispersion at high ionic concentrations was more pronounced in the presence of SCN^- than in the presence of Cl^- (Fig. 2a). Supporting this result, the electrostatic interaction energy between CHI-NH_3^+ and CS in the system containing SCN^- was lower than that in the system containing Cl^- (Fig. 5b). There is a systematic trend of PEC stability against ions in the Hofmeister series: highly chaotropic ions tend to break intrinsic ion pairs [35,39]. Thus, this result was considered valid. Furthermore, it was suggested that the chaotropic anions affect not only the charged groups but also the polar groups within the PECs because the electrostatic interaction energy between deprotonated CHI (CHI-NH_2) and CS forming complexes (Fig. S11) also showed lower values in the presence of SCN^- compared that in the presence of Cl^- (Fig. S12). This might be explained by the inhibition of the interaction involving polar groups because SCN^- is strongly adsorbed on polar groups owing to its high polarizability [24,25,82].

Comparing CS/CHI particles in concentrated and diluted dispersions, the diameter of the CS/CHI particles in the concentrated dispersion increased at a lower ionic concentration than that in the diluted dispersion. Generally, in concentrated dispersions, colloidal particles are assumed to be close to each other and are easily affected by attractive forces from neighboring particles [74]. As such, the particles in the concentrated dispersion tend to form aggregates and increase in diameter.

It is well known that the hydrophobicity of PECs is affected by ions, depending on their hydrated properties [36]. To investigate the specific ion effects on the microenvironmental hydrophobicity of the CS/CHI particles, the loading efficiency of CBB dyes as an indicator of adsorbed amounts and change in their λ_{max} was monitored. Indeed, CBB has been widely used as a probed to detect the microenvironmental hydrophobicity [83–85]. At low ionic concentrations, the loading efficiency of the CBB dye in CS/CHI particles with NaCl was higher than that with NaSCN (Fig. 3a). Meanwhile, at high ionic concentrations, the loading efficiency of dyes in CS/CHI particles with NaSCN was higher than that with NaCl. ζ-potential measurements showed that the surface charge of the CS/CHI particles decreases with the addition of salt (Fig. 2). Contrary to the prediction that the addition of ions would reduce the loading efficiency of CBB in CS/CHI particles since the electrostatic interaction between

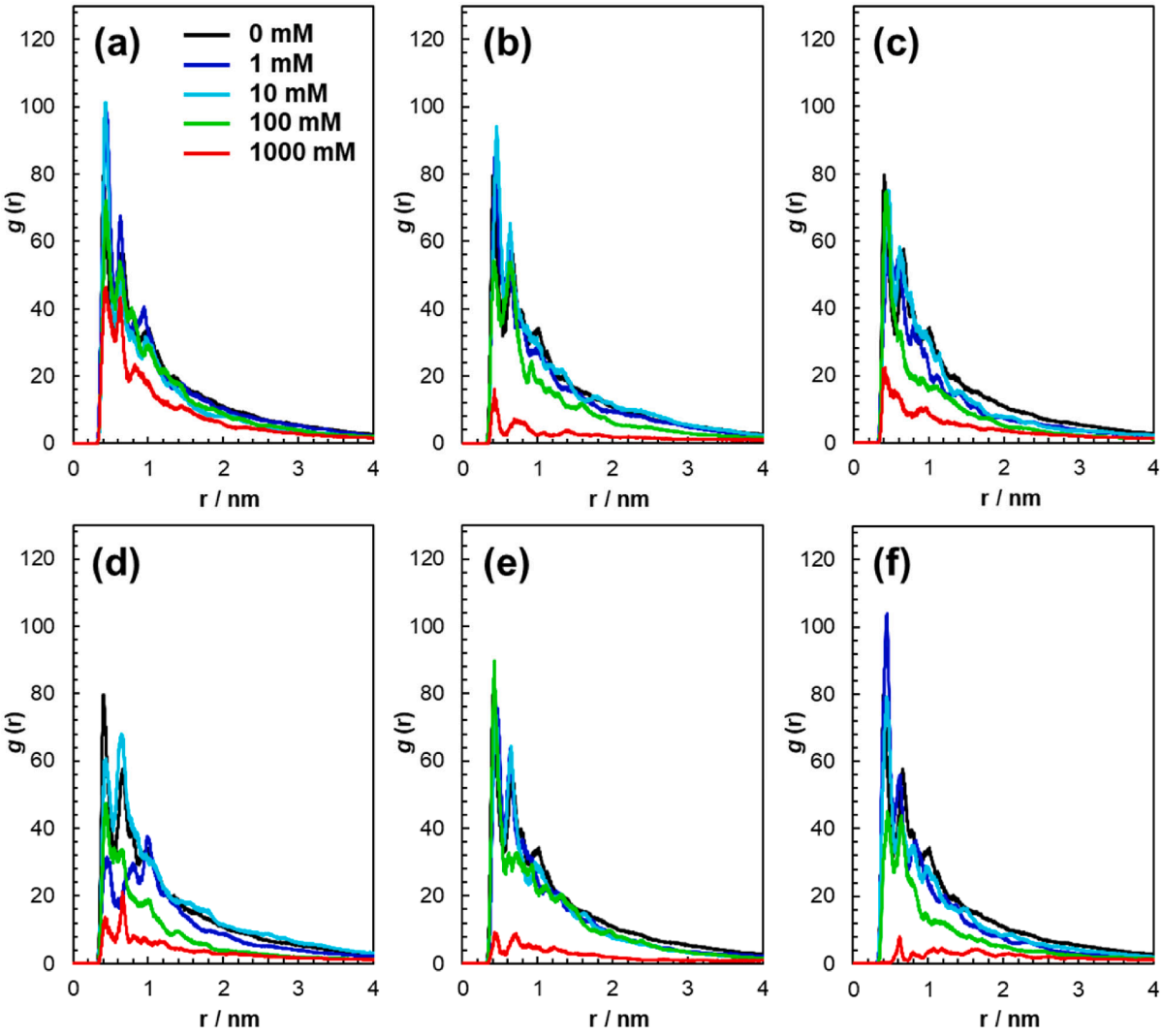

Fig. 8. RDFs of C atoms at 6-position of CS surrounding C atoms at 6-position of CHI-NH_3^+ in the systems of CHI-NH_3^+ and CS with NaCl (a), NaBr (b), $NaNO_3$ (c), NaI (d), $NaClO_4$ (e), and NaSCN (f) at different concentration.

CBB, which is an anionic dye and positively charged CS/CHI particles would decrease, the loading efficiency increased as the ionic concentration increased. This means that the interaction except electrostatic interaction between the CBB dye and CS/CHI particles is promoted by ions. It is well known that CBB with six aromatic rings interact with proteins or micelles via hydrophobic interaction. Therefore, it can be considered that the hydrophobicity the CS/CHI particles was enhanced by ions, resulting in the promotion of hydrophobic interaction with the CBB dye. This is corroborated by Fig. 3b, which shows the shift of λ_{max} of CBB towards longer wavelengths in the system containing both NaCl and NaSCN. This indicated that the microenvironmental hydrophobicity of the CS/CHI particles increased in the presence of ions. To identify the cause of the change in hydrophobicity, it is necessary to divide the hydrophobic domains of the PECs into several parts. Considering the unique structure of PEC particles, which exhibit hydrophobic cores surrounded by hydrophilic shells, it can be expected that the hydrophobicity is strengthened by the increase of (i) charge compensation of excess PE [21] consisting of shells, and the increase of (ii) the intrinsic ion pair between oppositely charged PEs [86] or (iii) the hydrophobic interaction between hydrophobic groups [87] within cores. For the CS/CHI particles, (i) corresponds to the compensation of $-NH_3^+$ in CHI with anions. (ii) is related to the intrinsic ion pair between $-NH_3^+$ in CHI and $-OSO_3^-$ and $-COO^-$ in CS. (iii) is applicable to the hydrophobic interaction between the hydrophobic groups (CH_n groups) in CHI and CS. The effects of ionic species and concentration on (i-iii) were analyzed based on the RDFs calculated from the MD simulation results.

Regarding (i), it was confirmed that chaotropic anions more closely contacted the $-NH_3^+$ of CHI than kosmotropic anions (Fig. 6). This means that chaotropic anions tend to form extrinsic ion pairs with $-NH_3^+$ compared to kosmotropic anions, which is consistent with previous experimental results that the less hydrated chaotropic ions more strongly bind to PEs [22,88].

As for (ii), the peak values of RDFs of $-NH_3^+$ of CHI-NH_3^+ surrounding $-OSO_3^-$ and $-COO^-$ of CS in the systems containing chaotropic anions are smaller than those in the systems containing kosmotropic anions (Figs. 7, S9), indicating that chaotropic anions broke the intrinsic ion pairs between $-NH_3^+$ of CHI and $-COO^-$ or $-OSO_3^-$ of CS more strongly than kosmotropic anions. Site-specific models theorize that when the formation of PECs is endothermic, salt ions prefer to break the intrinsic ion pairs [35,39]. Conversely, when the formation of PECs is exothermic, the salt ion acts have a preference to act as ions that remain unassociated with PEs, which are termed co-ions, and not to break the ion pairs [35,39]. There is a difference in the enthalpy generated during complexation between the monovalent anions. Yang et al. discovered that the changes in the enthalpy of complexation (ΔH) of PECs are negative or nearly zero with Cl^- or Br^-, respectively, whereas ΔH is positive for both I^- and ClO_4^- [35,39]. Therefore, it could be assumed that kosmotropic anions remained as co-ions, while chaotropic anions

destroyed the ion pair within CS/CHI. At high ionic concentrations, the RDF peak value decreased, regardless of the ion species (Fig. 7). This means that although kosmotropic anions prefer to act as co-ions, they destroy the intrinsic ion pairs. This might be explained by PEC dissolution by counterions through the screening effect at sufficiently high ionic concentrations [89].

With reference to (iii), the interaction between the hydrophobic groups was inhibited by all kinds of ions as their concentration increased (Figs. 8, S10). In particular, chaotropic anions are more likely to decrease hydrophobic interactions than kosmotropic anions. Kosmotropic anions stabilize the hydrophobic interactions of macromolecules by stabilizing the structure of water molecules, whereas chaotropic anions destabilize hydrophobic interactions by disrupting the structure of water molecules [90]. Therefore, it can be considered that kosmotropic anions are less effective than chaotropic anions in inhibiting hydrophobic interactions between CHI and CS.

Based on the analysis described above, it is suggested that the mechanism of enhancing the hydrophobicity of CS/CHI particles differs depending on the ionic species (Fig. 9a). Specifically, kosmotropic anions increase hydrophobicity by weakly compensating for the charge of excess CHI and maintaining intrinsic ion pairs and hydrophobic interactions. In contrast, chaotropic anions weaken intrinsic ion pairs and hydrophobic interactions; however, they increase hydrophobicity by causing charge neutralization of the excess charges of CHI.

At dilute ionic concentrations (<0.25 mM), the loading efficiency of the CBB dye was significantly higher and its λ_{max} was significantly shifted toward longer wavelengths in the system containing NaCl compared to that containing NaSCN (Fig. 3). The λ_{max} of CBB shifts from 584 nm in hydrophilic media to 618 nm in hydrophobic media [91]. Because the λ_{max} of CBB in the CS/CHI particle dispersion in the absence of salts was 585 nm, CS/CHI particles can be regarded as hydrophilic. Hydrated Cl^- can accumulate on the positively charged and hydrophilic surfaces of particles with structured water layers [19], compensating for the charge of CHI and increasing its hydrophobicity. Conversely, SCN^- is excluded from the water shell layers [19] and has difficulty entering the CS/CHI particles. However, at a concentrated ionic concentration (2.5 mM), as shown in Fig. 3, the loading efficiency of the CBB dye was significantly higher and its λ_{max} was significantly shifted toward longer wavelengths in the system containing NaSCN compared to that containing NaCl. This might be explained by the increase in hydrophobicity

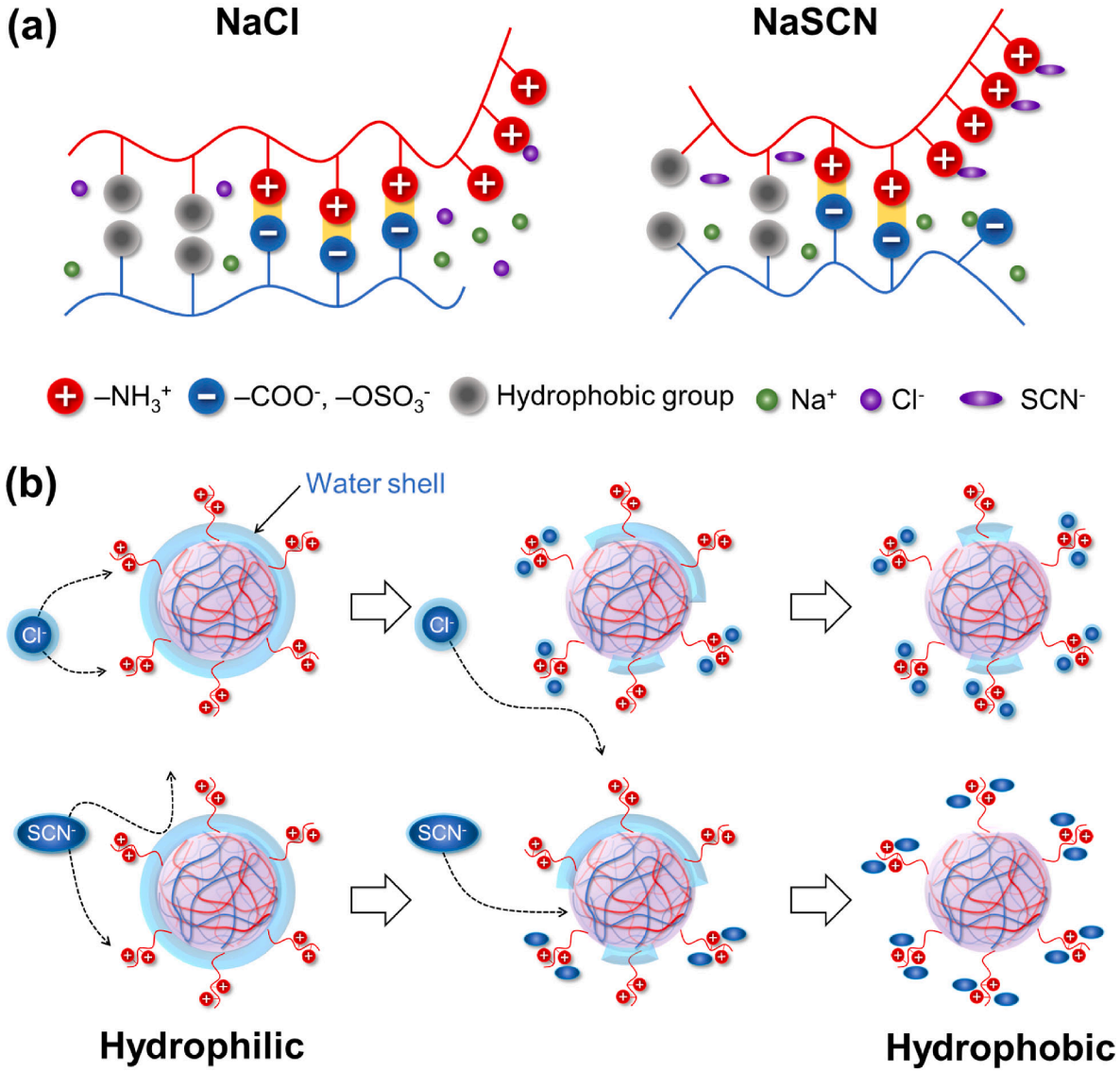

Fig. 9. (a) Schematic illustration of intrinsic ion pairs, extrinsic ion pairs, and hydrophobic interactions between CHI and CS in the presence of NaCl and NaSCN. (b) The effects of Cl^- and SCN^- on the hydrophilicity or hydrophobicity of CS/CHI particles associated with the change of hydration shell and the formation of extrinsic ion pair with $–NH_3^+$ and anions in CS/CHI particles.

of the CS/CHI particles due to charge compensation by counterions, as shown in Fig. 9b. Because chaotropic anions are more likely to accumulate on positively charged and hydrophobic surfaces than kosmotropic ions [19], their adsorption on CS/CHI particles is promoted, resulting in an increase in the hydrophobicity of the particles by compensating for the excess charge of CHI [21].

To consider whether these ion effects on hydrophilic PEC particles are commonly observed, the integration behavior of TPP and CHI particles, referred to as TPP/CHI particles, will be introduced as a representative example. The disintegration of TPP/CHI particles, in which chitosan and TPP are ionic cross-linked, was more strongly caused by kosmotropic ions than chaotropic ions because the kosmotropic ions more readily accumulate on the water layers of particles and disintegrate them [19]. Interestingly, the order of ions that induced the disintegration of TPP/CHI particles was $NO_3^- > Cl^- > SCN^-$, which was almost opposite to that of the CS/CHI particles. This means that there is a difference in hydrophilicity between the TPP/CHI and CS/CHI particles. Yeh et al. experimentally demonstrated a lower water content of CS/CHI particles than that of TPP/CS particles, indicating that CS/CHI particles exhibit a higher degree of ionic cross-linking [14]. It is well known that the lower the water content of the PECs, the stronger the ionic interaction between oppositely charged PEs [92]. Considering that the CS/CHI particles showed a lower water content than the TPP/CHI particles, it can be suggested that the ionic interaction in CS/CHI is stronger than that in TPP/CHI. In addition, there is a correlation between ionic interaction strength and dehydration [36]. Therefore, CS/CHI particles are expected to be more strongly dehydrated and hydrophobic than the TPP/CHI particles. PEC particles are usually described as colloids comprising hydrophobic cores surrounded by hydrophilic shells of polar noncomplex PE segments [93]. Comparing the TPP/CHI and CS/CHI particles, both seem to exhibit hydrophilic shells composed of ammonium ions; however, the CS/CHI particles are thought to have a more hydrophobic core, as mentioned above. Chaotropic ions can adsorb on the hydrophobic surface of colloids [19] and penetrate the hydrophobic region [94], whereas kosmotropic ions hardly adsorb on the surface of hydrophobic colloids [19,95]. Hence, the hydrophobicity of the cores of the TPP/CHI and CS/CHI particles seems to differ, which might lead to the disagreement of ionic order that causes the aggregation or disintegration of the PEC particles. Specifically, chaotropic ions accumulated on the strongly hydrophobic core of the CS/CHI particles and were excluded from the weakly hydrophobic cores of the TPP/CHI particles. In contrast, kosmotropic ions would accumulate on the weakly hydrophobic cores of the TPP/CHI particles and are excluded from the strongly hydrophobic core of the CS/CHI particles. These considerations suggest that the ion effects on the aggregation of PEC particles are affected not only by the hydrophobicity of the PEC shell but also by the hydrophobicity of the PEC core.

5. Conclusion

The effects of the monovalent anions of the Hoffmeister series on the aggregation of PEC particles were studied. Chaotropic anions caused aggregation of CS/CHI particles more effectively than kosmotropic anions. Although hydrophilic colloidal particles are susceptible to aggregation by strongly hydrated kosmotropic anions, the aggregation of CS/CHI particles is promoted by weakly hydrated chaotropic anions because of the increase in their hydrophobicity through the formation of extrinsic ion pairs between ions and polysaccharides. These findings provide insights into improving the stability of PEC particles as DDS carriers. For example, the dehydration of PEC particles with a dehydrating agent, such as polyethylene glycol, might contribute to increasing their stability because the adsorption of kosmotropic ions that are abundant in the body [20] on particles could be suppressed.

CRediT authorship contribution statement

Makoto Yamazaki: Conceptualization, Methodology, Investigation, Writing – original draft, Visualization. **Makoto Yabe:** Methodology, Investigation. **Kazutoshi Iijima:** Conceptualization, Methodology, Supervision, Writing – review & editing, Project administration.

Declaration of Competing Interest

The authors declare that they have no known competing financial interests or personal relationships that could have appeared to influence the work reported in this paper.

Data availability

No data was used for the research described in the article.

Acknowledgement

The authors acknowledge Prof. Shoji Maruo (Yokohama National University) for the ζ-potential and particle size analysis. We thank Instrumental Analysis Center at Yokohama National University for the use of UV/vis spectrophotometer (V-560, JASCO Corp.).

Appendix A. Supplementary material

Supplementary data to this article can be found online at https://doi.org/10.1016/j.jcis.2023.04.030.

References

[1] B. Philipp, H. Dautzenberg, K.J. Linow, J. Kötz, W. Dawydoff, Polyelectrolyte complexes - recent developments and open problems, Prog. Polym. Sci. 14 (1989) 91–172, https://doi.org/10.1016/0079-6700(89)90018-X.
[2] A.S. Michaels, Polyelectrolyte complexes, J. Ind. Eng. Chem. 57 (1965) 32–40, https://doi.org/10.1021/ie50670a007.
[3] R.M. Fuoss, H. Sadek, Mutual interaction of polyelectrolytes, Science 110 (1949) 552–554, https://doi.org/10.1126/science.110.2865.552.
[4] J.D. Mendelsohn, C.J. Barrett, V.V. Chan, A.J. Pal, A.M. Mayes, M.F. Rubner, Fabrication of microporous thin films from polyelectrolyte multilayers, Langmuir 16 (2000) 5017–5023, https://doi.org/10.1021/la000075g.
[5] J. You, S. Xie, J. Cao, H. Ge, M. Xu, L. Zhang, J. Zhou, Quaternized chitosan/poly (acrylic acid) polyelectrolyte complex hydrogels with tough, self-recovery, and tunable mechanical properties, Macromolecules 49 (2016) 1049–1059, https://doi.org/10.1021/acs.macromol.5b02231.
[6] Q.F. Wang, J.B. Schlenoff, The polyelectrolyte complex/coacervate continuum, Macromolecules 47 (2014) 3108–3116, https://doi.org/10.1021/ma500500q.
[7] N. Bhardwaj, S.C. Kundu, Silk fibroin protein and chitosan polyelectrolyte complex porous scaffolds for tissue engineering applications, Carbohydr. Polym. 85 (2011) 325–333, https://doi.org/10.1016/j.carbpol.2011.02.027.
[8] H.V. Le, D. Le Cerf, Colloidal polyelectrolyte complexes from hyaluronic acid: preparation and biomedical applications, Small (2022) e2204283.
[9] J. van der Gucht, E. Spruijt, M. Lemmers, M.A. Cohen Stuart, Polyelectrolyte complexes: bulk phases and colloidal systems, J. Colloid Interface Sci. 361 (2011) 407–422, https://doi.org/10.1016/j.jcis.2011.05.080.
[10] H. Dautzenberg, J. Kriz, Response of polyelectrolyte complexes to subsequent addition of salts with different cations, Langmuir 19 (2003) 5204, https://doi.org/10.1021/la0209482.
[11] H. Dautzenberg, N. Karibyants, Polyelectrolyte complex formation in highly aggregating systems. effect of salt: response to subsequent addition of NaCl, Macromol. Chem. Phys. 200 (1999) 118–125, https://doi.org/10.1002/(SICI)1521-3935(19990101)200:1<118::AID-MACP118>3.0.CO;2-K.
[12] L. Zhao, M. Skwarczynski, I. Toth, Polyelectrolyte-based platforms for the delivery of peptides and proteins, ACS Biomater. Sci. Eng. 5 (2019) 4937–4950, https://doi.org/10.1021/acsbiomaterials.9b01135.
[13] Z.C. Soe, B.K. Poudel, H.T. Nguyen, R.K. Thapa, W. Ou, M. Gautam, K. Poudel, S. G. Jin, J.H. Jeong, S.K. Ku, H.G. Choi, C.S. Yong, J.O. Kim, Folate-targeted nanostructured chitosan/chondroitin sulfate complex carriers for enhanced delivery of bortezomib to colorectal cancer cells, Asian J. Pharm. Sci. 14 (2019) 40–51, https://doi.org/10.1016/j.ajps.2018.09.004.
[14] M.K. Yeh, K.M. Cheng, C.S. Hu, Y.C. Huang, J.J. Young, Novel protein-loaded chondroitin sulfate-chitosan nanoparticles: preparation and characterization, Acta Biomater. 7 (2011) 3804–3812, https://doi.org/10.1016/j.actbio.2011.06.026.
[15] K. Hagiwara, M. Nakata, Y. Koyama, T. Sato, The Effects of coating pDNA/chitosan complexes with chondroitin sulfate on physicochemical characteristics and cell transfection, Biomaterials 33 (2012) 7251–7260, https://doi.org/10.1016/j.biomaterials.2012.06.040.

[16] M. Yamazaki, K. Iijima, Fabrication and characterization of polysaccharide composite films from polyion complex particles, Polymers 12 (2020) 435, https://doi.org/10.3390/polym12020435.
[17] M. Yamazaki, K. Iijima, Analysis of the aggregation mechanism of chondroitin sulfate/chitosan particles and fabrication of hydrogel cell scaffolds, Int. J. Biol. Macromol. 210 (2022) 233–242, https://doi.org/10.1016/j.ijbiomac.2022.05.027.
[18] Y. Zhang, E. Yildirim, H.S. Antila, L.D. Valenzuela, M. Sammalkorpi, J. L. Lutkenhaus, The influence of ionic strength and mixing ratio on the colloidal stability of PDAC/PSS polyelectrolyte complexes, Soft Matter 11 (2015) 7392–7401, https://doi.org/10.1039/c5sm01184a.
[19] T. López-León, M.J. Santander-Ortega, J.L. Ortega-Vinuesa, D. Bastos-González, Hofmeister effects in colloidal systems: influence of the surface nature, J. Phys. Chem. C 112 (2008) 16060–16069, https://doi.org/10.1021/jp803796a.
[20] E. Puolanne, M. Halonen, Theoretical aspects of water-holding in meat, Meat Science 86 (2010) 151–165, https://doi.org/10.1016/j.meatsci.2010.04.038.
[21] K. Abe, M. Koide, E. Tsuchida, Hydrophobicities in the domains of polyelectrolytes, J. Polym. Sci., Polym. Chem. Ed. 15 (1977) 2469, https://doi.org/10.1002/pol.1977.170151016.
[22] M. Salomäki, P. Tervasmäki, S. Areva, J. Kankare, The hofmeister anion effect and the growth of polyelectrolyte multilayers, Langmuir 20 (2004) 3679–3683, https://doi.org/10.1021/la036328y.
[23] F. Hofmeister, Zur Lehre Von Der Wirkung Der Salze, Archiv f. experiment. Pathol. u. Pharmakol 24 (1888) 247, https://doi.org/10.1007/BF01918191.
[24] W. Kunz, Specific ion effects in colloidal and biological systems, Curr. Opin. Colloid Interface Sci. 15 (2010) 34–39, https://doi.org/10.1016/j.cocis.2009.11.008.
[25] V. Mazzini, V.S.J. Craig, Specific-ion effects in non-aqueous systems, Curr. Opin. Colloid Interface Sci. 23 (2016) 82–93, https://doi.org/10.1016/j.cocis.2016.06.009.
[26] H.I. Okur, J. Hladilkova, K.B. Rembert, Y. Cho, J. Heyda, J. Dzubiella, P.S. Cremer, P. Jungwirth, Beyond the hofmeister series: ion-specific effects on proteins and their biological functions, J. Phys. Chem. B 2017 (1997) 121, https://doi.org/10.1021/acs.jpcb.6b10797.
[27] P. Lo Nostro, B.W. Ninham, Hofmeister phenomena: an update on ion specificity in biology, Chem. Rev. 112 (2012) 2286–2322, https://doi.org/10.1021/cr200271j.
[28] L. Musilová, V. Kašpárková, A. Mráček, A. Minařík, M. Minařík, The behaviour of hyaluronan solutions in the presence of hofmeister ions: a light scattering, viscometry and surface tension study, Carbohydr. Polym. 212 (2019) 395–402, https://doi.org/10.1016/j.carbpol.2019.02.032.
[29] Y. Zhang, S. Furyk, D.E. Bergbreiter, P.S. Cremer, Specific ion effects on the water solubility of macromolecules: PNIPAM and the hofmeister series, J. Am. Chem. Soc. 127 (2005) 14505–14510, https://doi.org/10.1021/ja0546424.
[30] S.Z. Moghaddam, E. Thormann, The hofmeister series: specific ion effects in aqueous polymer solutions, J. Colloid Interface Sci. 555 (2019) 615–635, https://doi.org/10.1016/j.jcis.2019.07.067.
[31] A. Salis, B.W. Ninham, Models and mechanisms of hofmeister effects in electrolyte solutions, and colloid and protein systems revisited, Chem. Soc. Rev. 43 (2014) 7358–7377, https://doi.org/10.1039/c4cs00144c.
[32] V. Mazzini, G. Liu, V.S.J. Craig, Probing the hofmeister series beyond water: specific-ion effects in non-aqueous solvents, J. Chem. Phys. 148 (2018), 222805, https://doi.org/10.1063/1.5017278.
[33] B. Hribar, N.T. Southall, V. Vlachy, K.A. Dill, How ions affect the structure of water, J. Am. Chem. Soc. 124 (2002) 12302–12311, https://doi.org/10.1021/ja026014h.
[34] Y. Marcus, Effect of ions on the structure of water: structure making and breaking, Chem. Rev. 109 (2009) 1346–1370, https://doi.org/10.1021/cr8003828.
[35] M. Yang, Z.A. Digby, J.B. Schlenoff, Precision doping of polyelectrolyte complexes: insight on the role of ions, Macromolecules 53 (2020) 5465–5474, https://doi.org/10.1021/acs.macromol.0c00965.
[36] J.B. Schlenoff, A.H. Rmaile, C.B. Bucur, Hydration contributions to association in polyelectrolyte multilayers and complexes: visualizing hydrophobicity, J. Am. Chem. Soc. 130 (2008) 13589–13597, https://doi.org/10.1021/ja802054k.
[37] W. Kunz, P. Lo Nostro, B.W. Ninham, The present state of affairs with hofmeister effects, Curr. Opin. Colloid Interface Sci. 9 (2004) 1–18, https://doi.org/10.1016/j.cocis.2004.05.004.
[38] K.P. Gregory, G.B. Webber, E.J. Wanless, A.J. Page, Lewis strength determines specific-ion effects in aqueous and nonaqueous solvents, J. Phys. Chem. A 123 (2019) 6420–6429, https://doi.org/10.1021/acs.jpca.9b04004.
[39] J.B. Schlenoff, M. Yang, Z.A. Digby, Q. Wang, Ion content of polyelectrolyte complex coacervates and the donnan equilibrium, Macromolecules 52 (2019) 9149–9159, https://doi.org/10.1021/acs.macromol.9b01755.
[40] K. Sadman, Q. Wang, Y. Chen, B. Keshavarz, Z. Jiang, K.R. Shull, Influence of hydrophobicity on polyelectrolyte complexation, Macromolecules 50 (2017) 9417–9426, https://doi.org/10.1021/acs.macromol.7b02031.
[41] K.H. Shen, M. Fan, L.M. Hall, Molecular dynamics simulations of ion-containing polymers using generic coarse-grained models, Macromolecules 54 (2021) 2031–2052, https://doi.org/10.1021/acs.macromol.0c02557.
[42] S. Chen, Z.G. Wang, Driving force and pathway in polyelectrolyte complex coacervation, Proc. Natl. Acad. Sci. USA 119 (2022), https://doi.org/10.1073/pnas.2209975119.
[43] B. Kang, H. Tang, Z. Zhao, S. Song, Hofmeister series: insights of ion specificity from amphiphilic assembly and interface property, ACS Omega 5 (2020) 6229–6239, https://doi.org/10.1021/acsomega.0c00237.
[44] E.S. Dragan, S.S. Polyelectrolyte, V.I. Complexes, P. Structure, Polyanion molar mass and polyion concentration effects on complex nanoparticles based on poly (sodium 2-acrylamido-2-methylpropanesulfonate), J. Polym. Sci. A Polym. Chem. 42 (2004) 2495–2505, https://doi.org/10.1002/pola.20110.
[45] Y. Miyazaki, S. Yakou, K. Takayama, The investigation for the formation of complexes between opposite-charged dextran derivatives, J. Pharm. Sci. Technol. 61 (2001) 59–70, https://doi.org/10.14843/jpstj.61.59.
[46] Origin(Pro). Origin(Pro) Version Number (e.g. "Version 2021b"). OriginLab Corporation, Northampton, MA, USA, 2021.
[47] M.J. Abraham, T. Murtola, R. Schulz, S. Páll, J.C. Smith, B. Hess, E. Lindahl, GROMACS: high performance molecular simulations through multi-level parallelism from laptops to supercomputers, Softwares 1–2 (2015) 19–25, https://doi.org/10.1016/j.softx.2015.06.001.
[48] K.N. Kirschner, A.B. Yongye, S.M. Tschampel, J. González-Outeiriño, C.R. Daniels, B.L. Foley, R.J. Woods, GLYCAM06: a generalizable biomolecular force field. Carbohydrates, J. Comput. Chem. 29 (2008) 622–655, https://doi.org/10.1002/jcc.20820.
[49] M.D. Hanwell, D.E. Curtis, D.C. Lonie, T. Vandermeersch, E. Zurek, G.R. Hutchison, Avogadro: an advanced semantic chemical editor, visualization, and analysis platform, J. Cheminform. 4 (2012) 17, https://doi.org/10.1186/1758-2946-4-17.
[50] A.W. Sousa da Silva, W.F. Vranken, ACPYPE – AnteChamber PYthon Parser interface, BMC Res. Notes 5 (2012) 367, doi: 10.1186/1756-0500-5-367.
[51] C. Cadena, E.J. Maginn, Molecular simulation study of some thermophysical and transport properties of triazolium-based ionic liquids, J. Phys. Chem. B 110 (2006) 18026–18039, https://doi.org/10.1021/jp0629036.
[52] X. Liu, S. Zhang, G. Zhou, G. Wu, X. Yuan, X. Yao, New force field for molecular simulation of Guanidinium-based ionic liquids, J. Phys. Chem. B 110 (2006) 12062–12071, https://doi.org/10.1021/jp060834p.
[53] R.R. Kumal, P.N. Wimalasiri, M.J. Servis, A. Uysal, Thiocyanate ions form antiparallel populations at the concentrated electrolyte/charged surfactant interface, J. Phys. Chem. Lett. 13 (2022) 5081–5087, https://doi.org/10.1021/acs.jpclett.2c00934.
[54] R. Salomon-Ferrer, D.A. Case, R.C. Walker, An overview of the amber biomolecular simulation package, WIREs Comput. Mol. Sci. 3 (2013) 198–210, https://doi.org/10.1002/wcms.1121.
[55] W.L. Jorgensen, J. Chandrasekhar, J.D. Madura, R.W. Impey, M.L. Klein, Comparison of simple potential functions for simulating liquid water, J. Chem. Phys. 79 (1983) 926–935, https://doi.org/10.1063/1.445869.
[56] T. Darden, D. York, L. Pedersen, Particle mesh Ewald: an N·log(N) method for ewald sums in large systems, J. Chem. Phys. 98 (1993) 10089–10092, https://doi.org/10.1063/1.464397.
[57] B. Hess, H. Bekker, H.J. Berendsen, J.G. Fraaije, LINCS: a linear constraint solver for molecular simulations, J. Comput. Chem. 18 (1997) 1463–1472.
[58] G. Bussi, D. Donadio, M. Parrinello, Canonical sampling through velocity rescaling, J. Chem. Phys. 126 (2007) 14101, https://doi.org/10.1063/1.2408420.
[59] M. Parrinello, A. Rahman, Crystal structure and pair potentials: a molecular-dynamics study, Phys. Rev. Lett. 45 (1980) 1196–1199.
[60] R. Fletcher, M.A. Powell, A rapidly convergent descent method for minimization, Comput. J. 6 (1963) 163–168, https://doi.org/10.1093/comjnl/6.2.163.
[61] The PyMOL Molecular Graphics System, Version 2.0 Schrödinger, LLC.
[62] M.C. Gurau, S.M. Lim, E.T. Castellana, F. Albertorio, S. Kataoka, P.S. Cremer, On the mechanism of the hofmeister effect, J. Am. Chem. Soc. 126 (2004) 10522–10523, https://doi.org/10.1021/ja047715c.
[63] P.C. Hiemenz, Rajagopalan, R. Principles of Colloid and Surface Chemistry, Dekker, New York, 1997.
[64] B.I.M. Wicky, S.L. Shammas, J. Clarke, Affinity of IDPs to their targets is modulated by ion-specific changes in kinetics and residual structure, Proc. Natl. Acad. Sci. U.S.A. 114 (2017) 9882–9887, https://doi.org/10.1073/pnas.1705105114.
[65] I.B. Ivanov, R.I. Slavchov, E.S. Basheva, D. Sidzhakova, S.I. Karakashev, Hofmeister effect on micellization, thin films and emulsion stability, Adv. Colloid Interface Sci 168 (2011) 93–104, https://doi.org/10.1016/j.cis.2011.06.002.
[66] Y. Zhang, P.S. Cremer, The inverse and direct hofmeister series for lysozyme, Proc. Natl. Acad. Sci. U.S.A. 106 (2009) 15249–15253, https://doi.org/10.1073/pnas.0907616106.
[67] M. Boström, D.F. Parsons, A. Salis, B.W. Ninham, M. Monduzzi, Possible origin of the inverse and direct hofmeister series for lysozyme at low and high salt concentrations, Langmuir 27 (2011) 9504–9511, https://doi.org/10.1021/la202023r.
[68] F. Ding, Z. Tang, B. Ding, Y. Xiong, J. Cai, H. Deng, Y. Du, X. Shi, Tunable thermosensitive behavior of multiple responsive chitin, J. Mater. Chem. B 2 (2014) 3050, https://doi.org/10.1039/c4tb00067f.
[69] I. Russo Krauss, D. Cavasso, D. Ciccarelli, R.K. Heenan, O. Ortona, G. D'Errico, L. Paduano, A hofmeister series perspective on the mixed micellization of cationic and non-ionic surfactants, J. Mol. Liq. 335 (2021), 116205, https://doi.org/10.1016/j.molliq.2021.116205.
[70] T. López-León, J.L. Ortega-Vinuesa, D. Bastos-González, Ion-Specific aggregation of hydrophobic particles, ChemPhysChem 13 (2012) 2382–2391, https://doi.org/10.1002/cphc.201200120.
[71] T. López-León, A.B. Jódar-Reyes, D. Bastos-González, J.L. Ortega-Vinuesa, Hofmeister effects in the stability and electrophoretic mobility of polystyrene latex particles, J. Phys. Chem. B 107 (2003) 5696–5708, https://doi.org/10.1021/jp0216981.
[72] A. Kiriy, J. Yu, M. Stamm, Interpolyelectrolyte complexes: a single-molecule insight, Langmuir 22 (2006) 1800–1803, https://doi.org/10.1021/la051908b.
[73] C. Vauthier, B. Cabane, D. Labarre, How to concentrate nanoparticles and avoid aggregation? Eur. J. Pharm. Biopharm. 69 (2008) 466–475, https://doi.org/10.1016/j.ejpb.2008.01.025.
[74] T. Tadros, Interparticle interactions in concentrated suspensions and their bulk (rheological) properties, Adv. Colloid Interface Sci. 168 (2011) 263–277, https://doi.org/10.1016/j.cis.2011.05.003.

[75] A.F. Thünemann, M. Muller, H. Dautzenberg, J.F. Joanny, H. Lowen, Polyelectrolyte complexes, Adv. Polym. Sci. 166 (2004) 113–171, https://doi.org/10.1007/b11350.
[76] T. Delair, Colloidal polyelectrolyte complexes of chitosan and dextran sulfate towards versatile nanocarriers of bioactive molecules, Eur. J. Pharm. Biopharm. 78 (2011) 10–18, https://doi.org/10.1016/j.ejpb.2010.12.001.
[77] H. Dautzenberg, Polyelectrolyte complex formation in highly aggregating systems. 1. Effect of salt: polyelectrolyte complex formation in the presence of NaCl, Macromolecules 30 (1997) 7810–7815, https://doi.org/10.1021/ma970803f.
[78] A.D. Kulkarni, Y.H. Vanjari, K.H. Sancheti, H.M. Patel, V.S. Belgamwar, S. J. Surana, C.V. Pardeshi, Polyelectrolyte complexes: mechanisms, critical experimental aspects, and applications, Artif. Cell Nanomed. Biotechnol. 44 (2016) 1615–1625, https://doi.org/10.3109/21691401.2015.1129624.
[79] A. Zintchenko, G. Rother, H. Dautzenberg, Transition highly aggregated complexes soluble complexes via polyelectrolyte exchange reactions: kinetics, structural changes, and mechanism, Langmuir 19 (2003) 2507–2513, https://doi.org/10.1021/la0265427.
[80] C. Schatz, J.-M. Lucas, C. Viton, A. Domard, C. Pichot, T. Delair, Formation and properties of positively charged colloids based on polyelectrolyte complexes of biopolymers, Langmuir 20 (2004) 7766–7778, https://doi.org/10.1021/la049460m.
[81] J. Požar, D. Kovačević, Complexation between polyallylammonium cations and polystyrenesulfonate anions: the effect of ionic strength and the electrolyte type, Soft Matter 10 (2014) 6530, https://doi.org/10.1039/C4SM00651H.
[82] Y.Y. Zhan, Q.C. Jiang, K. Ishii, T. Koide, T. Kobayashi, O. Kojima, S. Takahashi, S. Tachikawa, S. Uchiyama, S. Hiraoka, Polarizability and isotope effects on dispersion interactions in water, Commun. Chem. 2 (2019) 141, https://doi.org/10.1038/s42004-019-0242-0.
[83] T. Akagi, K. Watanabe, M. Akashi, H. Kim, Stabilization of polyion complex nanoparticles composed of poly(amino acid) using hydrophobic interactions, Langmuir 26 (2010) 2406, https://doi.org/10.1021/la902868g.
[84] C. Samsonoff, J. Daily, R. Almog, D.S. Berns, The use of coomassie brilliant blue for critical micelle concentration determination of detergents, J. Colloid Interface Sci. 109 (1986) 325, https://doi.org/10.1016/0021-9797(86)90310-3.
[85] X. Zhu, J. Wu, W. Shan, W. Tao, L. Zhao, J.-M. Lim, M. D'Ortenzio, R. Karnik, Y. Huang, J. Shi, O.-C. Farokhzad, Polymeric nanoparticles amenable to simultaneous installation of exterior targeting and interior therapeutic proteins, Angew. Chem., Int. Ed. Engl. 55 (2016) 3309–3312, https://doi.org/10.1002/anie.201509183.
[86] R. Koehler, R. Steitz, R. von Klitzing, About different types of water in swollen polyelectrolyte multilayers, Adv. Colloid Interface Sci. 207 (2014) 325–331, https://doi.org/10.1016/j.cis.2013.12.015.
[87] M. Yang, S.L. Sonawane, Z.A. Digby, J.G. Park, J.B. Schlenoff, Influence of "Hydrophobicity" on the composition and dynamics of polyelectrolyte complex coacervates, Macromolecules 55 (2022) 7594–7604, https://doi.org/10.1021/acs.macromol.2c00267.
[88] R.A. Ghostine, R.F. Shamoun, J.B. Schlenoff, Doping and diffusion in an extruded saloplastic polyelectrolyte complex, Macromolecules 46 (2013) 4089–4094, https://doi.org/10.1021/ma4004083.
[89] M. Skepö, P. Linse, Dissolution of a polyelectrolyte-macroion complex by addition of salt, Phys. Rev. E: Stat. Phys., Plasmas, Fluids, Relat. Interdiscip. Top. 66 (2002), 051807, https://doi.org/10.1103/PhysRevE.66.051807.
[90] G. Salvi, P. De Los Rios, M. Vendruscolo, Effective interactions between chaotropic agents and proteins, Proteins 61 (2005) 492–499, https://doi.org/10.1002/prot.20626.
[91] C. Duval-Terrié, J. Huguet, G. Muller, Self-assembly and hydrophobic clusters of amphiphilic polysaccharides, Colloids Surf. A Physicochem. Eng. Asp. 220 (2003) 105–115, https://doi.org/10.1016/S0927-7757(03)00062-1.
[92] J. Fu, H.M. Fares, J.B. Schlenoff, Ion-pairing strength in polyelectrolyte complexes, Macromolecules 50 (2017) 1066–1074, https://doi.org/10.1021/acs.macromol.6b02445.
[93] H.V. Le, V. Dulong, L. Picton, D. Le Cerf, Polyelectrolyte complexes of hyaluronic acid and diethylaminoethyl dextran: formation, stability and hydrophobicity, Carbohydr. Polym. 292 (2022), 119711, https://doi.org/10.1016/j.colsurfa.2021.127485.
[94] J.N. Sachs, T.B. Woolf, Understanding the Hofmeister Effect in Interactions between Chaotropic Anions and Lipid Bilayers: Molecular Dynamics Simulations, J. Am. Chem. Soc. 125 (2003) 8742–8743, https://doi.org/10.1021/ja0355729.
[95] D.M. Kolb, C. Franke, Surface-States at the Metal Electrolyte Interface, Appl. Phys. A 49 (1989) 379–387, https://doi.org/10.1007/BF00615020.